Important declarations

Please remove this info from manuscript text if it is also present there.

Associated Data

Data not supplied by the author for this reason:
Submitted article is a literature review paper, no experiments were conducted and no source code developed.

Required Statements

Competing Interest statement:
The authors declare that they have no competing interests.

Funding statement:
This work was supported by the project Development of SCSS-Net: Solar Corona Structures Segmentation algorithm by deep neural networks, within 1st Slovak RPA call under ESA Contract No. 4000143601/24/NL/MH/mp

Solar corona structures detection and segmentation using deep neural networks - a survey

Peter Butka [1], **Martin Sarnovsky** [Corresp., 1], **Viera Kresnakova** [1], **Lenka Kaliskova** [1], **Lubomir Lazor** [1], **Simon Mackovjak** [2]

[1] Department of Cybernetics and Artificial Intelligence, Technical University in Kosice, Kosice, Slovakia

[2] Institute of Experimental Physics, Department of Space Physics, Slovak Academy of Sciences, Kosice, Slovakia

Corresponding Author: Martin Sarnovsky
Email address: martin.sarnovsky@tuke.sk

Solar image segmentation and detection are a critical part of solar physics research. In recent years, deep learning-based techniques have proven to be effective for various solar image processing tasks. Modern methods based on novel deep learning architectures are often performing better in comparison to other traditional machine learning or computer vision methods. In this paper, we provide a review of current approaches of deep learning methods in specific area of solar image data analysis - detection and segmentation techniques of coronal holes and active regions. The paper introduces the image segmentation and detection methods, both traditional and modern ones, based on deep-learning. Subsequently, we provide a systematic overview of current deep learning approaches to segmentation and detection of coronal holes and active regions. In particular, we discuss the potential applications of the methods in solar science research, emphasizing its adaptability to different solar data types and its contribution to advancing automated solar feature detection techniques.

Solar corona structures detection and segmentation using deep neural networks - a survey

Peter Butka[1], Martin Sarnovsky[1], Viera Kresnakova[1], Lenka Kaliskova[1], Lubomir Lazor[1], Simon Mackovjak[2]

[1] Department of Cybernetics and Artificial Intelligence, Faculty of Electrical Engineering and Informatics, Technical University of Kosice, Letna 9, 040 01, Kosice, Slovakia

[2] Department of Space Physics, Institute of Experimental Physics, Slovak Academy of Sciences, Watsonova 47, 040 01, Kosice, Slovakia

Corresponding Author:

Martin Sarnovsky[1]

Technical University of Kosice, Letna 9, 040 01, Kosice, Slovakia

Email address: martin.sarnovsky@tuke.sk

Solar corona structures detection and segmentation using deep neural networks - a survey

Peter Butka[1], Martin Sarnovsky[1], Viera Kresnakova[1], Lenka Kaliskova[1], Lubomir Lazor[1], and Simon Mackovjak[2]

[1]**Department of Cybernetics and Artificial Intelligence, Faculty of Electrical Engineering and Informatics, Technical University of Kosice, Letna 9, 040 01, Kosice, Slovakia**
[2]**Department of Space Physics, Institute of Experimental Physics, Slovak Academy of Sciences, Watsonova 47, 040 01, Kosice, Slovakia**

Corresponding author:
Martin Sarnovsky[1]

Email address: martin.sarnovsky@tuke.sk

ABSTRACT

Solar image segmentation and detection are a critical part of solar physics research. In recent years, deep learning-based techniques have proven to be effective for various solar image processing tasks. Modern methods based on novel deep learning architectures are often performing better in comparison to other traditional machine learning or computer vision methods. In this paper, we provide a review of current approaches of deep learning methods in specific area of solar image data analysis - detection and segmentation techniques of coronal holes and active regions. The paper introduces the image segmentation and detection methods, both traditional and modern ones, based on deep learning. Subsequently, we provide a systematic overview of current deep-learning approaches to segmentation and detection of coronal holes and active regions. In particular, we discuss the potential applications of the methods in solar science research, emphasizing its adaptability to different solar data types and its contribution to advancing automated solar feature detection techniques.

INTRODUCTION

Solar activity is the primary driver of changes in space conditions. Space weather cannot be understood or reliably predicted without continuous and automated monitoring of structures and events originating in the atmosphere of the Sun. Today, continuous acquisition of solar images is ensured by space-based telescopes that image the dynamic solar atmosphere with unprecedented spatial, temporal, and spectral resolution. The challenge, raised in recent years, is to process the increasingly large amount of generated data and automatically extract all important information from the images obtained by these instruments (Aschwanden, 2010; Pérez-Suárez et al., 2011).

To effectively understand and predict space weather events, accurate identification and characterization of solar structures over long periods are essential. Missions such as SOHO (Domingo et al., 1995), SDO (Pesnell et al., 2012), Solar Orbiter (Müller, D. et al., 2020), and Parker Solar Probe (Fox et al., 2016) provide significant amounts of data that require automated methods for the detection and segmentation of solar corona structures. Meanwhile, deep learning architectures have proved their increase in quality of segmentation results in different domains and have found their way also into the domain of solar observations. Continuous enhancements in machine learning models for solar image segmentation are crucial for embedding these observations into real-time space weather forecasting systems. The significance of automated monitoring and forecasting has been emphasised by recent extreme space weather events. For example, the severe geomagnetic storm in May 2024 (Spogli, 2024) highlighted the potential threats such events pose to critical infrastructure.

Upcoming space-based telescopes, like the European Space Agency's Vigil mission (Palomba and Luntama, 2022), are designed to improve solar weather monitoring from Lagrange Point 5 (L5), thereby

offering early alerts for possible space weather risks. The expected amount of data from Vigil and related initiatives highlights the need for sophisticated machine learning techniques to effectively analyze and derive valuable insights from solar data. Therefore, it is an important step to prepare for new data, analyze, and investigate all aspects related to the use of new instruments. Such an analysis should include both a better understanding of the data to be produced and methods for their processing. The first aspect was analyzed in (Majirsky et al., 2025), where the authors identified instruments from operating space missions that monitor Space Weather activity and are relevant for data-driven studies for the planned deep space mission Vigil, created a list of the most extreme events that caused great or severe geomagnetic storms in the last 30 years and the methodology for their identification, including tools with visualization of related solar structure images for events during long period of previous missions. However, for better preparation of the Vigil mission, another important aspect is review and analysis of existing segmentation and detection techniques. Therefore, this review provides an overview of existing strategies for segmenting and detecting solar corona structures. We compare various methods, noting their strengths and limitations, including traditional and deep learning methods.

The remainder of this paper is organized as follows. The following section describes the rationale and intended audience of the survey conducted. The search methodology is then described. In the following section, we provide a general overview of image segmentation techniques, including traditional and modern methods based on deep learning. Then, we describe an overview of segmentation and detection techniques of solar images. The main findings of the survey are summarized in discussion and conclusion sections.

RATIONALE AND INTENDED AUDIENCE

Image processing and computer vision are in their golden era thanks to deep learning. In recent years, algorithms for automatic image classification, detection, and segmentation based on deep neural networks have significantly outperformed traditional approaches, mostly based on predefined rules. They are so reliable and effective that they are routinely employed in common life applications. This is mainly due to three reasons: a) the huge amount of images available for training of neural networks; b) available high-performance computation resources; and c) accessible software frameworks for the straightforward development of deep learning models. Although all these conditions are met in the space weather domain, the ordinary exploitation of machine learning techniques in this domain is still in its initial phase (Camporeale et al., 2018).

The survey carried out represents an overview of currently used segmentation and detection methods applied in the domain of solar corona structures. The motivation for such activity is the need for space weather centres and space weather researchers to develop powerful tools and algorithms for processing images operationally and with a good level of accuracy in order to extract automatically relevant information and characteristics of solar corona structures that are the source of space weather activity. Deep analysis of existing approaches helps to understand the current state of the art and main developments in this area during recent years.

The survey is intended to support academic and industry researchers working on deep learning in the domain of solar structure identification. We hope that our results inspire researchers to explore new methods in close cooperation with relevant domain experts. In addition, we expect practitioners to see the potential and benefits of deep learning models and will contribute their knowledge and experience to the final quality of the models.

SEARCH METHODOLOGY

In this chapter, we provide an analysis of the current status of solar structure segmentation and detection, considered as a domain-specific state-of-the-art analysis. For the literature review, we followed a methodological approach and used ParsifAl[1] for support in the selection of existing approaches.

To perform a proper state-of-the-art analysis, we used ParsifAl, an online tool that is used to help researchers perform systematic literature reviews while also providing them with a way to document the entire process. We started by defining research questions that were based on our tasks. Then these questions were put into context by applying a PICOC method. This method specifically helps clarify research and systematic review of the literature. It is usually used to form research questions, but because

[1] https://parsif.al/

they were predefined in our case, we used it to get suitable keywords. Each letter in the name PICOC represents an area that you should not forget about while doing a literature review. The individual areas are as follows: Population, Intervention, Comparison, Outcome, and Context.

As a result of this method, we ended up with five strong points based on which we were able to identify the relevant keywords, knowing that we would not neglect any part of our goals. ParsifAl also helped us to gather our selection criteria for the articles. Articles would have to be in English, available online, and published in less than 8 years. Then we selected the sources in the form of online databases, including Scopus and ArXiv, with ArXiv used for preprints. Then we formulated the relevant queries and imported the articles with their abstracts into ParsifAl. We obrained the initial set of papers using two queries, the first one was more general: *("segmentation") AND ("active regions" OR "coronal holes") AND ("solar") AND ("SDO" OR "SOHO").* The second query was more specifically aimed towards deep learning methods: *("segmentation" OR "detection") AND ("active regions" OR "coronal holes") AND ("solar") AND ("SDO" OR "SOHO") AND ("deep learning").* We examined each of the articles to determine whether they were relevant for our work or not. The queries also returned a review article (Reiss et al., 2021), which also had a newer preprint (Reiss et al., 2024) available. We decided to use both of these review articles, and since they were well documented, we also decided to include some older methods even if those were not returned by the queries because of the publication year criterion. In addition to the segmentation techniques, we also included papers related to detection if we found them interesting due to their specific method, data, or evaluation techniques. Also, some papers used the term detection instead of segmentation, but we used the correct term in the summarised table. However, for the final selection of suitable techniques, papers on segmentation are the most important and we preferably focused on them.

We ended up with 39 different papers, which we analyse further in this chapter. ParsifAl also has a method for a brief summary of the articles called a data extraction form. We used this tool to make the final version of Table 1, which gives us a quick overview of the different approaches we found during our analysis.

GENERAL OVERVIEW OF SEGMENTATION TECHNIQUES

Image segmentation is a fundamental technique in computer vision that aims to partition digital images into regions (segments) that share similar visual characteristics. By delineating images into more homogeneous and clearly defined segments, subsequent tasks (such as object recognition or feature extraction) can be performed with greater accuracy and efficiency (Abdulateef and Salman, 2021).

There are a variety of strategies for image segmentation, ranging from classical feature-based approaches to more advanced methods driven by deep learning. Traditional methods often rely on elementary features, such as pixel intensity or color, to determine boundaries within images. In contrast, machine learning-based approaches, especially deep learning, leverage large annotated datasets to learn the inherent patterns of objects and backgrounds. While conventional techniques rely on hand-crafted features, deep neural networks automatically extract hierarchical features that are more robust to variations in illumination, viewpoint, and noise (Ronneberger et al., 2015).

Image segmentation is indispensable in numerous domains. In medical imaging, it helps delineate organs and pathologies for diagnosis and treatment planning. In robotics, it facilitates obstacle detection, localization, and object manipulation. In remote sensing, it enables identification of land features and anomalies. Its remarkable adaptability and precision make image segmentation a cornerstone of modern computer vision research and applications.

Although image segmentation, object detection, and image classification are closely related, each serves a different purpose.

- Object detection focuses on locating instances of predefined object classes within an image, often by drawing bounding boxes around them (Redmon et al., 2016). This approach identifies the approximate positions of objects but does not delineate their precise boundaries.

- Image segmentation extends object detection by providing pixel-level delineation for each object or region of interest (Zaitoun and Aqel, 2015). Segmentation models produce masks that accurately outline the boundaries of objects, offering finer detail regarding shape, size, and spatial extent.

Table 1. Overview of analysed papers related to solar structures segmentation and detection models, or related task for generation or translation. Event types are: AR - Active regions, CH - Coronal Holes, SS - Sunspots, All - all three types. DL column: Y/N, if deep learning was/was-not used. Full name of papers or method's acronyms are available in Table 2.

Short Name	Task	Event	DL	Image Waveband	Reference
DLMSED	Detection	CH	Y	193 Å, 304 Å, Intensitygram (SDO)	(Baek et al., 2021)
MSMT-CNN	Detection	AR	Y	171 Å, 195 Å, 284 Å, 304 Å, 3934 Å, Magnetogram (SOHO)	(Almahasneh et al., 2022)
MWSED	Detection	AR/CH	Y	131 Å, 171 Å, 193 Å	(Kucuk et al., 2017)
SARDL	Detection	AR	Y	LOS magnetogram	(Quan et al., 2021)
SDUYOLO	Detection	SS	Y	H-alpha	(Santos et al., 2023)
SETDRN	Detection	AR/CH	Y	SDO/HMI, SDO/AIA (band not specified)	(Sarker and Banda, 2019)
DLSIC	Detection & Generation	All	Y	94Å, 131Å, 171Å, 193Å, 304Å, 211Å, Intensitygram (SDO)	(Baek et al., 2024)
RDGT	Detection & tracking	AR	Y	SDO/HMI, LOS magnetograms	(Gong et al., 2024)
ARSAR	Segmentation & Detection	AR	N	LOS magnetogram	(Yan-mei et al., 2021)
ACWE	Segmentation	CH	N	193 Å	(Boucheron et al., 2016)
ACWE-2	Segmentation	CH	N	193 Å	(Grajeda et al., 2023)
ADPSAR	Segmentation & Detection	AR	N	193 Å	(Sukarsih et al., 2020)
ARUSM	Segmentation	AR/CH	N	171 Å, 193 Å	(Arish et al., 2016)
ASDSIS	Segmentation & Detection	SS	Y	SDO HMI continuum	(Mourato et al., 2024)
CATCH	Segmentation	CH	N	193 Å	(Heinemann et al., 2019)
CHARM	Segmentation	CH	N	193 Å, LOS magnetogram	(Krista and Gallagher, 2009)
CHIMERA	Segmentation	CH	N	171 Å, 193 Å, 211 Å, LOS magnetogram	(Garton et al., 2018)
CHIPS	Segmentation	CH	N	171 Å, 193 Å, 211 Å	(Reiss et al., 2024)
CHMAP (EZSEG)	Segmentation	CH	N	193 Å (SDO), 195 Å (STEREO)	(Caplan et al., 2016)
CHORTLE	Segmentation	CH	N	193 Å, LOS magnetogram	(Lowder et al., 2014)
CHRONNOS	Segmentation	CH	Y	94 Å, 131 Å, 171 Å, 193 Å, 211 Å, 304 Å, 335 Å	(Jarolim et al., 2021)
CNN193	Segmentation	CH	Y	193 Å	(Illarionov and Tlatov, 2018)
CNN193-2	Segmentation	CH	Y	193 Å	(Illarionov et al., 2020)
FEDCM	Segmentation	CH	N	193 Å	(Bandyopadhyay et al., 2020b)
ICHUML	Segmentation	CH	N	171 Å, 193 Å, 211 Å	(Inceoglu et al., 2022)
MIDM	Segmentation	CH	N	193 Å	(Caplan et al., 2023)
PORACM	Segmentation	CH	N	193 Å	(Bandyopadhyay et al., 2020a)
RTSIC	Segmentation	AR/CH	N	94 Å, 131Å, 195 Å, 171 Å, 284 Å, 304 Å, H-alpha	(Hughes et al., 2019)
SCSS-Net	Segmentation	AR/CH	Y	171 Å, 193 Å	(Mackovjak et al., 2021)
SPoCA-CH	Segmentation	AR/CH	N	193 Å	(Verbeeck et al., 2014)
SPoCA-HEK	Segmentation	AR/CH	N	193 Å	(Delouille et al., 2018)
SUNSCC	Segmentation	SS	Y	White light	(Sayez et al., 2023)
SYNCH	Segmentation	CH	N	171 Å, 193 Å, 304 Å	(Hamada et al., 2018)
WWWBCS	Segmentation	AR/CH	N	171 Å, 193 Å, 211 Å	(Reiss et al., 2024)
GMSOI	Generation	AR	Y	193 Å	(Cherti et al., 2023)
CEVAE	Translation	AR/CH	Y	171 Å	(Giger and Csillaghy, 2024)
ETLSC	Translation	AR/CH	Y	94 Å, 171 Å, 193 Å, 211 Å	(Salvatelli et al., 2022)
GANS	Translation	AR/CH	Y	304 Å, LOS magnetogram	(Dash et al., 2022)
ITIT	Translation	All	Y	Various sources and channels	(Jarolim et al., 2024)

Table 2. Acronyms and full names of method abbreviations or title of selected papers characterized in Table 1.

Acronym	Full Name
ACWE, ACWE-2	Active Contours Without Edges (original, and 2nd Iteration)
ARSAR	Automatic Recognition of Solar Active Regions
ADPSAR	Automatic Detection Process of Solar Active Regions
ASDSIS	Automatic Sunspot Detection Through Semantic and Instance Segmentation
CATCH	Collection of Analysis Tools for Coronal Holes
CEVAE	Context-Encoding Variational Autoencoder
CHART	Coronal Hole Automated Recognition and Tracking
CHIPS	Coronal Hole Identification using a Probabilistic Scheme
CHIMERA	Coronal Hole Identification via Multi-thermal Emission Recognition Algorithm
CHARM	Coronal Hole Automated Recognition and Monitoring
CHORTLE	Coronal Hole Observer and Regional Tracker for Long-term Examination
CHRONNOS	Coronal Hole RecOgnition Neural Network Over multi-Spectral-data
CHMAP/EZSEG	Coronal Hole Mapping and Analysis Pipeline
CNN193, CNN193-2	CNN193 method based on CNNs by Illarionov et al., original and second iteration
DLSIC	Deep Learning-Based Solar Image Captioning
DLMSED	Deep-Learning-Based Methods for Solar Event Detection
ETLSC	Exploring the Limits of Synthetic Creation
FEDCM	Fuzzy Energy-Based Dual Contour Method
GANS	Generative Adversarial Networks
GMSOI	Generative Models for High Resolution Solar Observation Imaging
ICHUML	Identification of Coronal Holes Using Unsupervised Machine Learning
ITIT	Instrument to Instrument Translation
MIDM	Minimum Intensity Disk Merge
MSMT-CNN	MultiSpectral-MultiTask-CNN
MWSED	Multi-Wavelength Solar Event Detection Using Faster R-CNN
PORACM	Parameterized Online Region-Based Active Contour Method
RDGT	ReDetGraphTracker
RTSIC	Real-Time Solar Image Classification
SCSS-Net	Solar Corona Structures Segmentation by Deep Learning
SDUYOLO	Sunspot Detection Using YOLOv5
SARDL	Solar Active Region Detection Using Deep Learning
SETDRN	Solar Event Tracking with Deep Regression Networks
SPoCA-CH, SPoCA-HEK	Spatial Possibilistic Clustering Algorithm
SUNSCC	Segmenting, Grouping and Classifying Sunspots From Ground-Based Observations Using Deep Learning
SYNCH	Synoptic Coronal Hole Maps
WWWBCS	Warwick wavelet watershed-based coronal segmentation

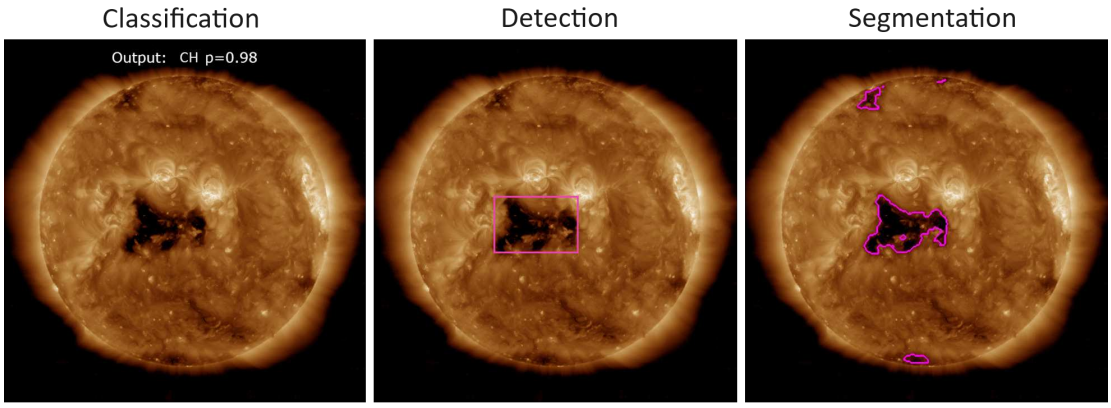

Figure 1. Comparison of classification, detection and segmentation tasks.

- Image classification treats an image holistically, assigning it to one of several predefined categories (Krizhevsky et al., 2012). In this task, the primary goal is to determine which class an image belongs to, without localizing or outlining any objects within it.

Fig.1 shows the differences of the mentioned approaches in the solar coronal hole detection use case.

Traditional Image Segmentation Techniques

Before the advent of deep learning, image segmentation largely relied on methods that were conceptually straightforward but limited in their ability to handle complex scenes.

- Thresholding: This technique categorizes pixels based on intensity values relative to one or more thresholds, effectively converting images into binary (or multi-level) forms. Although thresholding is computationally efficient, its performance degrades in scenarios where the foreground and background share similar intensity distributions (Sezgin and Sankur, 2004).

- Edge Detection: By identifying abrupt changes in pixel intensity or color, edge detection methods delineate object boundaries within an image (Canny, 1986). These methods perform well when clear gradients define the edges of objects. However, they can struggle in complex or noisy environments where boundaries are faint or overlapping.

Although traditional segmentation techniques laid an essential foundation, their capacity to handle intricate objects and variations in lighting, color, and texture remains limited. This paved the way for more robust solutions based on machine learning and deep neural networks, which continue to advance state-of-the-art performance in image segmentation.

Deep Learning Image Segmentation Approaches

The emergence of deep learning has brought about a major shift in the field of image segmentation. Traditional rule-based techniques have been largely supplanted by data-driven methods capable of learning highly complex feature representations. Convolutional Neural Networks (CNNs) in particular have demonstrated remarkable success in capturing both low- and high-level image features, enabling unprecedented accuracy and adaptability (Lecun et al., 2015). This section highlights prominent deep learning models and architectures that have shaped modern segmentation, discussing both their fundamental principles and their practical applications.

U-Net, first introduced by Ronneberger et al. (2015), was designed primarily for biomedical image segmentation. Its signature U-shaped architecture comprises a contracting path (encoder) and an expanding path (decoder). The contracting path captures contextual information through successive convolution and pooling operations, while the expanding path performs transposed convolutions (upsampling) to recover spatial resolution. Skip connections between corresponding layers of the encoder and decoder

preserve high-resolution features, which are critical for accurate boundary delineation. Figure 2 provides an overview of the original U-Net design.

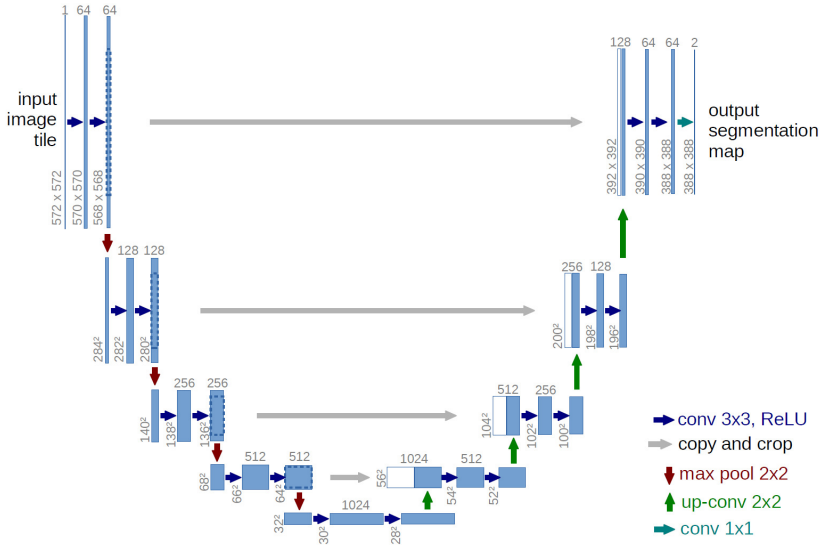

Figure 2. Schematic diagram of the U-Net architecture.

Due to its efficacy and relatively modest data requirements, U-Net has found broad adoption in applications ranging from medical imaging to remote sensing. Several notable extensions and variants have since been proposed:

- U-Net++: This variant introduces dense skip connections to narrow the semantic gap between the feature maps of the encoder and the decoder, thus improving the precision of the segmentation (Zhou et al., 2018).
- Attention U-Net: By incorporating an attention mechanism, this model selectively focuses on relevant parts of the input image, enabling more precise segmentation of structures that vary in size and clarity (Oktay et al., 2018).
- 3D U-Net: Designed for volumetric data, 3D U-Net employs three-dimensional convolutions for enhanced spatial context in applications such as MRI and CT scans (Çiçek et al., 2016).
- MultiResUNet: This variant leverages multi-resolution blocks to capture features across different scales, thus improving its adaptability to diverse image domains (Ibtehaz and Rahman, 2020).

These progressive refinements underscore U-Net's versatility and its continued importance as a foundational architecture in modern segmentation research.

The YOLO ("You Only Look Once") series has been instrumental in real-time object detection, and recent iterations, such as YOLOv8 [2] , further refine these capabilities. Although YOLOv8 is designed primarily for detection, it has notable implications for segmentation by laying a solid foundation for region-of-interest identification.

Key innovations in YOLOv8 include deeper architectures for more discriminative feature extraction and carefully optimized computational pathways. Pruning and quantization techniques reduce redundant computations while preserving high accuracy, making YOLOv8 well-suited for latency-sensitive applications (Redmon et al., 2016). By improving detection accuracy and efficiency, YOLOv8 complements segmentation workflows in scenarios where precise region proposals are critical.

Generative Adversarial Networks (GANs) (Goodfellow et al., 2014) have opened new frontiers in image processing and synthesis. Among their notable applications is Pix2Pix (Isola et al., 2017), which employs a conditional GAN framework for image-to-image translation tasks. In a typical segmentation

[2]https://github.com/ultralytics/ultralytics

context, Pix2Pix can learn to map an input image to a desired segmentation mask, effectively treating it as a translation problem.

Pix2Pix adopts a U-Net-like structure in the generator and a patch-based discriminator, focusing on local regions to enhance detail fidelity. Although it requires paired training data, subsequent methods such as CycleGAN (Zhu et al., 2017) relax this requirement by introducing a cycle consistency loss, allowing translations in the absence of paired datasets. These advances have broadened the scope of GAN-based models, making them versatile tools for tasks such as style transfer, domain adaptation, and synthetic data generation for segmentation. Examples of applications in different domains can be found in (Roy et al., 2023; Gadari et al., 2023; van der Schot et al., 2023; Patel et al., 2023).

The DeepLab family of models (Chen et al., 2017, 2018) is recognized for introducing atrous (dilated) convolutions to address multi-scale context in semantic segmentation. By modulating the receptive field without reducing feature-map resolution, atrous convolutions enable the network to capture both fine details and broader contextual cues. DeepLabV3 and DeepLabV3+ also incorporate atrous spatial pyramid pooling (ASPP), which probes the input at multiple scales and significantly improves performance on objects of varying sizes.

Based on the Faster Region-Based Convolutional Neural Network (R-CNN) framework (Ren et al., 2015), Mask R-CNN (He et al., 2017) refines the pipeline to perform instance segmentation. In a two-stage process, candidates are first proposed and then, for each region, a bounding box, class label, and segmentation mask are simultaneously predicted. This integrated approach has proven highly effective for tasks that require pixel-level object delineation, such as autonomous driving and robotics.

From the landmark introduction of U-Net for biomedical segmentation to the real-time object detection prowess of YOLO and the generative capabilities of Pix2Pix, deep learning has fundamentally altered how segmentation tasks are approached. Modern architectures excel not only in capturing and preserving spatial details, but also in managing scale variations, contextual relationships, and even the synthesis of new training data.

As researchers continue to refine existing models and propose novel architectures, several trends promise to shape the next phase of segmentation research. These include leveraging self-supervision for reduced labeling demands, integrating transformers for global context modeling, and combining generative networks with traditional CNN-based approaches to further enhance performance. Collectively, these innovations signal a rapidly evolving field poised to deliver increasingly robust and flexible solutions to a growing array of real-world segmentation challenges.

OVERVIEW OF SEGMENTATION AND DETECTION TECHNIQUES IN SOLAR IMAGES

In the following subsections, we provide an overview of the basic characteristics of the following approaches: segmentation, detection, and other approaches.

Overview of segmentation approaches

In the article (Boucheron et al., 2016) the approach to segmentation of the coronal holes does not lie in absolute intensity values. The algorithm assumes that coronal holes have more homogeneous intensities than the surrounding active regions and quiet Sun, which should lead to improved consistency with varying datasets. Segmentation is performed on full-disk Extreme Ultraviolet (EUV) images obtained from Solar Dynamics Observatory's Atmospheric Imaging Assembly (SDO/AIA) decimated from 4096×4096 pixels to 512×512 pixels. Detected coronal holes align well with unipolar magnetic regions and are consistent with concurrent solar wind observations.

In 2023, researchers investigated this study more thoroughly (Grajeda et al., 2023). There are 3 main differences present. The translation of the Active Contours Without Edges (ACWE) algorithm from MATLAB to Python is the major one, with the choice of homogeneity parameters and the use of different seeding parameters being the other two.

The study presented in (Heinemann et al., 2019) is not a fully automated method. The process of detecting the boundaries of coronal holes is automated, but all of the detected regions need to be checked by a human. The extraction of coronal hole boundaries is done with a modulated intensity threshold method, which is performed on a separate user-friendly graphical user interface. The input consists of EUV images from SDO/AIA down-scaled from the original 4096×4096 pixels to 1024×1024 pixels with the effects on segmentation due to down-scaling being negligible.

The study (Krista and Gallagher, 2009) detects coronal holes using a histogram-based intensity thresholding technique and subsequently analyses their characteristics in relation to fast solar wind streams at three distinct locations within the heliosphere. The algorithm was tested on 195Å EUV images from STEREO-SECCHI/EUVI and Solar and Heliospheric Observatory's Extreme ultraviolet Imaging Telescope (SOHO/EIT) instruments, X-ray pictures aboard Hinode's X-ray Telescope (XRT), and magnetograms from SOHO/SDI. These full-disk images were used in full resolution and transformed into Lambert's equal-area projection (LEAP) maps and then partitioned into a series of overlapping subimages from which local histograms were extracted. The threshold of the low-intensity regions was determined by the histograms, and the regions were then classified as coronal holes or filaments using magnetograms from the SOHO/MDI. Across all three different inputs, the thresholding algorithm consistently and successfully identified coronal hole boundaries. Compared with measurements of solar wind, they were at approximately 1 AU from ACE and STEREO. Findings reveal that flux tubes originating from coronal holes expand super-radially within 1 AU.

The paper (Garton et al., 2018) offers a novel approach. Coronal Hole Identification via Multi-thermal Emission Recognition Algorithm (CHIMERA) analyses multithermal EUV images obtained from the SDO/AIA with the addition of an Helioseismic and Magnetic Imager (HMI) magnetogram as LOS. It examines the intensity ratios across three different EUV wavebands, specifically the 171 Å, 193 Å, and 211 Å all at full resolution of 4096×4096 pixels. This allows CHIMERA to accurately identify and extract coronal hole boundaries and other properties such as area, position, latitudinal and longitudinal width, and magnetic polarity. These feature properties can be statistically compared with solar wind effects at 1 AU.

CHIPS or *Coronal hole identification using a probabilistic scheme* mentioned in the review article (Reiss et al., 2024) introduces a novel approach by assigning a probability to both detected coronal holes and their boundaries. The algorithm is trained to function on images from three different EUV wavebands, precisely the 171 Å, 193 Å, and 211 Å obtained from the SDO/AIA. These images undergo a 2D Gaussian filter to remove speckle and noise, after which comes the threshold identification and final detection of coronal holes on the greyscale EUV image converted to a binary one. Probability is calculated from the intensity values of the individual pixels by applying a sigmoid function, with an additional beta distribution, to estimate the parameters for regions with more than one pixel.

Another article (Caplan et al., 2016) focusses on the use of MATLAB to map coronal holes using synchronised EUV images from two separate wavebands. 193 Å from STEREO/EUVI A and B and 195 Å from SDO/AIA, with both sources being used with the same resolution of 2048×2048 pixels. These images are then preprocessed by Point Spread function Deconvolution (PSD) to enhance image quality and corrected by limb-brightening to try and reduce variation in intensity values as the model, like many others, relies on intensity thresholding. Finally, the images undergo an inter-instrument transformation, so that the intensities between them are normalised. The coronal holes are then detected, and the separate images are subsequently merged into EUV and coronal hole maps.

The study (Lowder et al., 2014) presents an automated thresholding method for tracking and detecting coronal holes and their boundaries. To do so, the algorithm uses full-disk EUV images from SOHO/EIT, SDO/AIA, and STEREO/EUVI accompanied by HMI and MDI magnetograms to calculate the area and magnetic flux of coronal holes. The model was trained on two different wavebands, 193 Å from SDO and 195 Å from both SOHO and STEREO, with better results coming from SDO and STEREO images. This discrepancy is attributed to a higher level of scattered light in the SOHO/EIT instrument measurements.

The paper (Jarolim et al., 2021) presents CNN for segmentation of full-disk maps of the boundaries of coronal holes in real time. It can do so on seven different EUV channels from the AIA and HMI magnetogram onboard the SDO. The wavebands included are 93 Å, 131 Å, 171 Å, 193 Å, 211 Å, 304 Å, and 335 Å scaled down to 512×512 pixels. The Coronal Hole RecOgnition Neural Network Over multi-Spectral-data (CHRONNOS) algorithm employs a region-growing multi-spectral encoder-decoder architecture, starting at an image resolution of 8×8 pixels, which progressively increases until it reaches a resolution of 512×512 pixels. The authors also demonstrated the importance of the individual EUV channels by training a SCAN model, that only detects coronal holes one waveband at a time. The CHRONNOS model was evaluated against an independent manually curated test set and showed good agreement with an Intersection-over-Union (IoU) of 0.63. It correctly detected 98.1% of the 261 coronal holes with an area greater than $1.5 \times 10^{10} km^2$ identified from November 2010 to December 2016. The model provides reliable coronal hole detections regardless of the level of solar activity and

exceeds human performance in terms of consistency and reliability. CHRONNOS performs best with combined channel information, but can also obtain coronal hole segmentation maps from line-of-sight (LOS) magnetograms alone. The proposed neural network provides users with reliable data for studying solar-cycle dependencies and coronal hole properties and is fit for real-time space weather applications.

CNN was also used in a study (Illarionov and Tlatov, 2018). With the segmentation of coronal holes heavily dependent on image thresholding and complex pre- and postprocessing, this approach tries to forego these nontrivial techniques. This CNN only takes one full-disk EUV channel 193 Å obtained from the SDO/AIA instrument and downsampled to just 256×256 pixels. The authors specifically examined the long-term fluctuations of coronal holes during solar cycle 24 and believe that this algorithm can outperform hand-engineered solar image analysis, while also demonstrating the stability of neural networks.

Research presented in (Illarionov et al., 2020) showed that the CNN based on the U-net architecture was able to perform very well in the segmentation of coronal holes. The images remained in the same waveband but were transformed into synoptic maps with a resolution of 720×360 pixels. Since the model was originally trained on 256×256 pixels, the synoptic maps were downscaled to 360×180 pixels with spatial padding applied to achieve a target size of 512×256 pixels. The model then processes these images to create segmentation masks and extracts a 360×180 pixel region from these masks to form the final output. This model further proved that it can detect coronal holes in any image type without adjustments. It showed that the neural network treats all images the same, regardless of shape or content, ensuring consistent segmentation results. Thus, it can interpret whole-disk images, partial-disk images, or synoptic maps equally well.

An article (Verbeeck et al., 2014) is based on fuzzy C-means (FCM) and probabilistic C-means (PCM) clustering techniques. It is trained to detect coronal holes and active regions and their properties on EUV images from SOHO/EIT, STEREO/EUVI, PROBA2/SWAP, and SDO/AIA. with the best results coming from 193 Å waveband from AIA. The Spatial Possibilistic Clustering Algorithm (SPoCA) suite allows for the extraction of long-time series of active regions and coronal holes properties while also enabling tracking of individual active regions and coronal holes over time. The ability to detect them on almost any source of images makes it a popular choice for comparison in many papers.

A further modified version of SPoCA, specifically the SPoCA-CH module, appeared in 2018 (Delouille et al., 2018). In this case, it is used to detect coronal holes. The data used in this study consisted of EUV channel 193 Å from SDO/AIA and H_α Filtergrams from the Kanzelhöhe Observatory in Austria were used for comparison. The detected regions were then mapped onto HMI LOS magnetograms. The refreshed algorithm was now more conservative with the detection to reduce false-positive cases and had a larger dataset available. As a result, the number of filaments detected as coronal holes was approximately 6% of all detections.

The algorithm Warwick wavelet watershed-based coronal segmentation (WWWBCS) mentioned in the review paper (Reiss et al., 2024) was developed by Verwichte and Foullon based on their previous work from 2006 (Foullon and Verwichte, 2006) that took advantage of the temperature sensitivity between the EUV waveband ratios. WWWBCS uses images of three full-disk EUV channels obtained from the SDO/AIA instrument downscaled to 512×512 pixels. The bands incorporated are specifically 171 Å, 193 Å, and 211 Å. The 171 Å and 211 Å passbands are normalized with respect to the exposure time and pointing to match the 193 Å channel. The images are then filtered using a continuous Mexican-Hat wavelet transform and then segmented into separate regions.

In the paper (Inceoglu et al., 2022), the authors focused on the use of unsupervised machine learning methods, particularly K-means clustering, for the automated detection of coronal holes in solar images. They tested single and multi-channel approaches on solar EUV images in 171, 193, and 211 Å, observed by the AIA/SDO instrument. A thresholding approach based on the fitted bimodal Gaussians to the probability densities of intensities for each channel on each date was used, with the following calculation of thresholds based on the mean and standard deviation of the local maximum at higher intensities. The K-means method was applied, with the optimum number of clusters based on the scree plot. They claimed that the K-means method, with all thresholding and pre/postprocessing enabled them to provide a flexible approach that dynamically responds to variations of intensities in solar images. The authors produced binary maps and compared them with those based on the Collection of Analysis Tools for Coronal Holes (CATCH) and SPOCA-HEK algorithms.

The best results were achieved for composite images using only 193 and 211 Å passband images,

closely followed by single-channel AIA 193, as generally expected by all other approaches. For quantitative analysis, they used IoU and TSS (true skill score), and also they found overlapping with CHRONNOS method. Unfortunately, CATCH is not one of the algorithms that was analysed in semiqualitative analysis with 29 images that contain annotation of both coronal holes and filaments (as defined in a comparative study in (Reiss et al., 2024), in which this study is not presented), due to the fact that CATCH had manually removed filaments. However, CHRONNOS showed good results there and this study has good overlap. Besides some scattering issues and the setup of a thresholding scheme for a new dataset, which might be more complicated for this unsupervised approach, the use of more wavelengths can be beneficial for our future work. Also, some of the pre/post-processing ideas with normalization of data can be useful to consider in our effort to move for the new instrument.

The article (Bandyopadhyay et al., 2020b) presents an approach for automated coronal hole detection in solar images captured by the SDO/AIA, for 193 Å. These images were in FITS format with a resolution of 512x512 pixels. The preprocessing steps involved enhancing the contrast and removing noise to improve the quality of the images prior to segmentation.

The proposed method Fuzzy Energy-Based Dual Contour Method (FEDCM) is based on a fuzzy-energy simulated dual contours approach. This technique combines fuzzy logic principles with energy-based contour evolution to accurately detect coronal holes. By incorporating grey-scale intensity information into the energy function, the algorithm can effectively identify coronal holes based on their unique features. The segmentation results obtained using FEDCM were compared with existing algorithms available in 2020, such as ACWE, CNN, SPoCA, and CHIMERA. The evaluation metrics included standard measures for segmentation such as Dice and IoU, which measure the overlap between the segmented coronal holes and ground-truth images. They also qualitatively inspected results and considered their approach as more accurate than other approaches in detecting coronal holes and minimizing misclassifications. However, it depends on expectations, the closest competitor to them is CHIMERA as it shows similar results according to precise and detailed boundary identification, but it may overestimate some parts of the structure and bring scattering issues, especially inside larger structures. The evolution of contours during the process might be interesting for post-processing in some cases, but it also brings the aforementioned problems.

The study (Arish et al., 2016) focuses on developing a robust unsupervised segmentation method for solar data analysis, specifically targeting active regions and coronal holes in EUV full-disk images obtained from the SDO/AIA at 171 Å and 193 Å wavelengths. The primary goal is to automate the process of identifying and delineating these solar features to facilitate research on solar dynamics and space weather phenomena.

To achieve this, the segmentation method leverages a Bayesian framework, integrating NL-means and cellular learning automata within a Markov random field model. By utilizing the Gibbs estimator for label and hyperparameter estimation, the algorithm samples labels from their posterior probability distribution, enabling the subdivision of solar regions into active regions and coronal holes. This approach improves the efficiency and accuracy of solar feature detection compared to manual selection methods.

The evaluation of the segmentation results involves a comprehensive analysis of the filling factors of active regions and coronal holes within a dataset spanning from 2010 to 2012. By comparing the outcomes of the automated segmentation with manual selection approaches, the study identifies false-positive detections and assesses the algorithm's performance in accurately identifying solar features. Additionally, the study discusses the potential applications of the segmentation method in solar physics research, emphasizing its adaptability to different solar data types and its contribution to advancing automated solar feature detection techniques.

The document (Caplan et al., 2023) focuses on the analysis of coronal holes using the Minimum Intensity Disk Merge (MIDM) method, which effectively captures more CH area than traditional synoptic thresholding methods. The MIDM algorithm minimises the obscuration of dark features by bright structures, leading to higher coronal hole area and open flux estimates. The method involves using multiple EUV images to generate a full Sun EUV map, highlighting dark structures for enhanced CH detection. The detection algorithm, EZSEG, applies intensity thresholds to identify CH regions, with tunable parameters for optimal detection.

Data sources include SDO/AIA 193 Å EUV images processed with a limb-brightening correction method. The images are used to create EUV maps using both synoptic and MIDM methods. The MIDM method relies on merging multiple EUV images to build a full Sun map, emphasising coronal holes

detection. The evaluation of results involves comparing CH detections from the synoptic and MIDM methods, highlighting differences in coronal hole boundaries and open flux estimates. The algorithm effectively detects obscured coronal holes by considering multiple LOS viewing perspectives.

The paper (Bandyopadhyay et al., 2020a) provides another method for segmentation of coronal holes based on SDO/AIA 193 Å channel, called Parameterized Online Region-Based Active Contour Method (PORACM). As a first step, the Hough transformation is used for initialisation contours for the coronal holes and also to help remove the off-disk pixels (background and solar limbs). Then, the region-based active contour method forces the contours to move towards the boundary of the region of interest (RoI) in order to detect coronal holes based on a certain energy function. After a number of iterations, based on predefined stopping criteria, the contour movement is stopped. The final position of the contour (the position where the contour sticks) is regarded as a boundary of coronal holes, and the region inside the final contour is considered a coronal hole segmentation result. The method was visually compared to CNN and CHIMERA , where authors claim better results than CNN and comparable to CHIMERA. The authors showed a comparison with the CNN approach and declared its main advantage in its computational performance. The visual comparison was very limited in this paper and provided only several examples.

The document (Hughes et al., 2019) discusses the importance of updating training data for solar thematic mapping to ensure long-term consistency. It emphasizes the need for real-time, low-latency data streams for accurate solar region identification. The study focuses on evaluating the performance of different algorithms for solar image segmentation, particularly the random forest algorithm, which outperforms Gaussian and mixture models in creating thematic maps. The document highlights the subjectivity of expert labelling and the importance of consensus criteria for accurate classification. In terms of data sources, the study uses real-time, low-latency data streams available at the National Oceanic and Atmospheric Administration (NOAA) for solar image analysis. It is important to mention that GOES/SUVI images, which we would like to use also in our activity, are used in their analysis and for solar thematic maps generation. Regarding pre-processing, the data collected for the study is separated into training and testing sets. The consensus expert images are used for training and evaluation, while individual labelling is not considered. The data is preprocessed by discarding pixels associated with ”unlabelled” regions where experts could not reach a consensus. Visual quality inspection is conducted for all images to ensure data integrity and accuracy in the pre-processing stage.

The method of segmentation or detection involves using machine learning algorithms such as the random forest model. Hyperparameter estimation is performed through a grid search using k-fold validation on the training set. The random forest model is optimised by tuning hyperparameters such as the number of trees in the forest, maximum depth, and minimum number of samples for a leaf node. This method ensures the accurate segmentation of solar images and the creation of thematic maps. The evaluation of the study results focuses on comparing the performance of different algorithms in creating thematic maps. The random forest algorithm demonstrates superior performance by maximising the F1 measure, a robust metric for class imbalance. The study also qualitatively analyses the results of the segmentation to provide spatial insights into the performance of each classifier. The evaluation process involves comparing the accuracy, precision, recall, the F1 measure, and the True Skill Statistic (TSS) of each classifier to determine their effectiveness in the segmentation of solar images.

The document (Sayez et al., 2023) discusses the SunSCC pipeline, focusing on sunspot segmentation, clustering, and classification tasks. The segmentation of CNNs was trained on ground-based white-light observations from the USET facility located at the Royal Observatory of Belgium. The whole pipeline consists of three blocks. The first block uses the version of the U-Net architecture to provide segmentation. The second block receives as input the segmentation from the first block and aggregates the detected sunspots into sunspot groups using a clustering method inspired by the mean-shift algorithm. Each identified sunspot group is provided along with an angular distance map to the third block. The latter constitutes a classification network designed to predict the McIntosh 3-component classification for sunspots. It is based on ResNet34, an image encoder, and three multi-layer perceptrons (MLPs) organised hierarchically. Each MLP is specialised in the classification of one component of the McIntosh system.

An advantage of keeping the three blocks as independent as possible makes them versatile for enhancements and reuse. In this paper, the authors provide an example of how to combine different tasks within one pipeline in an interesting modular way, from segmentation to very detailed classification according to domain-specific scheme. Moreover, the results showed a very good correspondence with manually classified sunspots. Considering that segmentation is a pixel-wise extension of detection, the

authors evaluated the segmentation model as a detection model. They used true positive, false positive, and false negative cases, leading to precision, recall, and the F1 score. They also analysed how different thresholding settings affect the results of segmentation.

In (Mourato et al., 2024) the authors provide details on the application of deep learning techniques for the automated detection of sunspots in solar images. The research aims at semantic and instance segmentation methods to enhance the accuracy and efficiency of sunspot detection. Even if the paper considers visible light images and sunspot detection, it brings a very good insight into the potential and applicability of deep learning architectures, which is important for any solar structures analysis.

The researchers used SDO photosphere images (HMI continuum) combined with sunspots, such as the Debrecen Photoheliographic Data (DPD) and the Helioseismic and Magnetic Imager Debrecen Data (HMIDD), which provide detailed information on sunspot positions and areas. The preprocessing steps involved creating semantic and instance segmentation masks for the solar images. Semantic masks are group-agnostic, assigning a single binary segmentation mask to each image to identify the presence of sunspots. However, instance segmentation masks treat each sunspot group as a separate instance, resulting in multiple binary segmentation masks for each image. The bounding boxes for each group were defined on the basis of the external pixel coordinates of the sunspots.

The authors used U-Net and Mask R-CNN, two convolutional neural network architectures, for sunspot detection through semantic and instance segmentation. To evaluate the performance of the segmentation models, the researchers employed metrics such as IoU for semantic segmentation and mean average precision (mAP) for instance segmentation. According to their results, deep learning approaches were proved to outperform previous approaches and should be considered as the main candidates for future developments in the processing of solar images.

The paper (Mackovjak et al., 2021) discusses the development of the first version of SCSS-Net, a deep learning model for segmenting solar corona structures. Data from AIA 171 Å and AIA 193 Å channels were used due to their visibility of active regions and coronal holes. The SCSS-Net segmentation model is inspired by the U-Net framework, a well-known encoder-decoder architecture. It consists of downscaling convolutional and upscaling deconvolutional blocks, incorporated dropouts, concatenate connections between blocks on their specific scales of details, and a sigmoid activation function for segmentation output, which classifies each pixel of the image as 0 or 1 based on the set threshold. For target annotations, different sources were used: SPoCA-HEK, CHIMERA, Region-growth algorithm, and custom annotations obtained using the crowdsourcing. The study presents an interesting comparison of annotations, how the segmentations are affected by their quality. One of the most important advantages of deep learning architecture is that manually created annotations might contain some errors; however, the algorithm is able to learn generally plausible and effective segmentation models overcoming annotation biases. Another interesting result of the analysis showed that if we have different annotations, from which one overestimates and the other underestimates boundaries, training of SCSS-Net with their combinations resulted in segmentations with better boundaries, as the model is able to find some middle-ground solutions. This might lead to the reuse of some other segmentation algorithms as inputs for future models that might increase quality using a similar approach, but we should be careful in the selection of annotation schemes and analysis of results. For quantitative analysis, IoU and Dice were used for the comparison of different versions of models.

As was emphasised in other papers, it is often not easy to compare segmentation results because of the lack of a larger annotation set that was confirmed to be correct by different researchers. Therefore, qualitative visual analysis is often considered. One of the efforts to have some comparison-enabled testing dataset is available in the review article (Reiss et al., 2024), which provides some middle-like approach with selected images and their characterisation for parts that should or should not be detected by the algorithm, leading to detection-like analysis.

Overview of detection approaches

In this sub-section, we provide a short overview of approaches that focused on the detection of solar structures and did not apply pixel-by-pixel segmentation in their outputs.

The paper (Baek et al., 2021) focusses on detecting sunspots, prominences, and coronal holes from SDO datasets using the single shot multibox detector (SSD) and the Faster R-CNN, showcasing their comparative results. This study stands out by creating labelled datasets from SDO data and employing advanced object detection algorithms to accurately detect solar events and their locations.

For the detection experiment, coronal holes, sunspots, and prominences as solar events were selected. These phenomena were chosen for their distinct features that are observable in the SDO/AIA and the HMI wavelengths. Full-disk SDO data from 2010 to 2019, available from the Korean Data Centre for SDO, were used. Data were sampled every 12 hours for sunspots and coronal holes, and every 4 hours for prominences. The authors converted the original FITS format images (4096×4096 pixels) to JPEG format (512×512 pixels) as the events were visible even at lower resolutions.

Each solar event, along with bounding boxes and labels, was manually identified by solar physics experts using the LabellImg annotation tool. To ensure accuracy, two experts cross-validated the dataset. The dataset consisted of 5085 coronal holes, 4383 sunspots, and 2926 prominences. For object detection SSD and Faster R-CNN models using ResNet-101 as the feature extractor were employed.

The study demonstrates the promise of SSD and Faster R-CNN for solar event detection, particularly for coronal hole and sunspot detection. Compared to previous work (Kucuk et al., 2017), the results showed a significant improvement, with an mAP of 76% for coronal holes.

The study (Kucuk et al., 2017) focuses on automated solar event detection using low-resolution solar images. It employs Faster R-CNN, a deep learning approach, to detect events such as active regions and coronal holes. The study utilizes images from the SDO/AIA, obtained through the Heliowiever platform, and event reports from the Heliophysics Event Knowledgebase (HEK) via the Integrated Solar Database (ISD).

The datasets consist of images and event reports sampled at hourly intervals, focusing on active regions and coronal holes events visible in wavelengths 131 Å, 171 Å, and 193 Å. Experimentation involves training and evaluation of datasets spanning 2012-2014 and 2015, respectively. Faster R-CNN with ResNet-101 is chosen for object detection due to its favorable accuracy/training time ratio. The study adapts the Faster R-CNN implementation from Tensorflow models, experimenting with different image resizing ratios and learning rate adjustments.

The results indicate a general detection accuracy between 26% and 28% mAP@0.5, with CH detection often outperforming AR detection. Transfer learning from a pre-trained model improves overall accuracy but reduces CH detection accuracy slightly. Lowering the image resolution to 1K pixels does not significantly affect the accuracy, suggesting efficiency gains in training time. Single-wavelength training at 193 Å yields lower accuracy compared to multi-wavelength training, emphasising the effectiveness of the multi-wavelength approach.

The study (Quan et al., 2021) compares the performance of two object detection models, YOLO and Faster R-CNN, in detecting solar active regions. Data from the HMI onboard the SDO and NOAA provide full-disk solar images and active region information, respectively. A total of 4645 labeled images from 2010 to 2017 are divided into training (2010-2015) and testing (2016-2017) sets. The authors take six bounding box priors of YOLO V3, (10×14), (23×27), (37×58), (81×82), (135×169), (344×319).

Feature extraction is crucial, with Faster R-CNN employing region-based CNN and YOLO using direct regression. For Faster R-CNN, a Region Proposal Network (RPN) generates object proposals, while YOLO predicts the bounding-box coordinates and classification labels directly. Both models undergo training with specific optimisation algorithms and loss functions. Evaluation metrics include true positive and true negative rates. The results show that YOLO V3 outperforms Faster R-CNN in accuracy and speed, with true positive and true negative rates increasing by 4% and 1%, respectively, and YOLO V3 processing images 8 times faster.

In (Santos et al., 2023), the researchers utilised data from the Geophysical and Astronomical Observatory of the University of Coimbra (OGAUC), which has maintained a solar activity monitoring system since 1926, capturing daily images of the Sun using a spectroheliograph. These images, stored digitally, form one of the largest solar image datasets globally, spanning nearly a century, except for days with poor weather conditions in Coimbra. Automatic methods for detecting and tracking sunspots in these images are crucial for efficient analysis and longitudinal studies.

A YOLOv5 network was trained using 2000 $H_\alpha$continuum images from solar cycle 24, achieving a maximum precision of 90%. Despite initial challenges due to the small dataset size, the model demonstrated learning capabilities, reaching a precision of 33.33% after 73 epochs. Various experiments were conducted using different training methods and datasets, revealing insights into model performance and training requirements.

The results showed that YOLO benefited from larger images without frames, with cropping significantly improving performance. Pre-processing techniques, such as contrast enhancement, did not

significantly enhance the results. Additionally, experiments with different YOLO models demonstrated that larger models achieved slightly better precision but required longer training times.

Compared to previous methods using OGAUC images, YOLOv5 exhibited slightly higher detection accuracy on a larger dataset. However, compared to studies using space-based images, precision was lower, highlighting the impact of the image source on detection performance. This work contributes by showcasing YOLO's effectiveness in sunspot detection from OGAUC images, achieving up to 90% precision.

In (Almahasneh et al., 2022), the authors proposed a framework called MultiSpectral-MultiTask-CNN (MSMT-CNN), that leverages multiple time-matched image bands to predict separate detection results for each band. It follows three key principles:

1. Performing individual image band extraction of unique features to learn independent features specific to each modality.

2. Aggregating learnt features from different bands using fusion operators to analyse interdependencies.

3. Generating separate results per image band based on a multi-task loss, allowing detection of different sections of 3D objects.

The data used in the experiments are: SOHO/EIT images (prepared with the EIT routines), SOHO/MDI magnetogram, and Spectrohelioograph data in 3934 Å from Paris-Meudon (PM/SH). The authors eliminated any prominences or solar eruptions by masking out all areas outside the solar disk. The contrast of SOHO/MDI magnetograms is enhanced by intensity rescaling. Contrast enhancement was not used on SOHO/EIT and PM/SH data, as it was found to have minimal effect on detection results.

MSMT-CNN is highly modular and flexible, accommodating any number of multi-spectral images and supporting various fusion strategies and backbone architectures. Framework employs a CNN as a feature extraction network, with parallel branches producing a feature map per image band. These maps are concatenated and analyzed by parallel modules per band using Faster RCNN's RPN and detection module. Experiments demonstrate improved performance over single-band detection, and late fusion shows superior results.

The paper (Sarker and Banda, 2019) focusses on solving an existing labelling cadence of 4 to 12 hours, which creates a gap between observations and continuous data streams. To address this, authors pioneered the use of deep regression networks to track AR and CH events. This approach, the first of its kind in solar event tracking, fills the gap by generating continuously labelled event trajectories.

The authors collected event records from the HEK and annotated solar images based on these records. The proposed deep regression network, based on the Generic Object Tracking Using Regression Networks (GOTURN) approach, was trained on pairs of subsequent frames to produce high-level representations for object tracking.

Using data from 2012 to 2018, the authors trained and evaluated three tracking models: active regions, coronal holes, and a combined AR-CH model. The AR model showed the highest performance, with an Intersection over Ground Truth (IoGT) area mean score of 0.5495.

In (Baek et al., 2024), the authors introduce a novel method for captioning solar images using a transformer-based deep learning approach. The authors also present the creation of a new dataset, DeepSDO description, tailored for training such captioning models. The dataset encompasses nine solar events, including sunspots, flares, and coronal holes, sourced from solar image data from the Korean Data Center for SDO and scripts from NASA's SDO gallery website.

The proposed approach involves training a deep learning-based image captioning model, specifically the meshed-memory transformer, on the DeepSDO description dataset. Experimental results demonstrate that the method surpasses existing benchmarks across four evaluation metrics. This research showcases the potential of deep learning-based image captioning in generating informative captions for various solar features, offering implications for solar physics and space weather research.

The proposed methodology involves utilizing the meshed-memory transformer algorithm and the DeepSDO description dataset, marking the first endeavor in solar image captioning. Authors leverage features extracted from solar images using a ResNet-based Faster R-CNN, feeding them as inputs to the M2 transformer to generate captions. The DeepSDO description dataset, a subset of the DeepSDO dataset,

comprises pairs of human-generated captions and corresponding JPG images sourced from a decade of SDO gallery data (2010-2019).

Through training, validation, and testing on the DeepSDO description dataset, the model demonstrates proficiency in generating captions for solar images. Performance evaluation using BLEU, METEOR, ROUGE, and CIDEr metrics validates the effectiveness of their approach.

Using SDO/HMI's high-resolution full-disk photospheric images, the authors of the study (Yan-mei et al., 2021) followed methods to automatically recognise active regions from HMI magnetograms. Comparison with National Oceanic and Atmospheric Adminstration's Space Weather Prediction Center (NOAA SWPC) compiled active regions from 2010 to 2018 revealed a strong correlation (0.87) between automatically recognised and SWPC active regions. Although the total number of automatically recognised active regions was slightly less than the SWPC's count, most unidentified active regions were small and lacked the potential for significant eruptions. This automatic recognition method directly provides real-time data for eruption prediction, which facilitates the operational application of eruption prediction models.

The resulting AR data, released as Space-weather HMI Active Region Patches (SHARP), have been instrumental in studying solar phenomena. Using HMI magnetogram data, the authors achieved automatic recognition of active regions, providing valuable data for solar activity prediction and study. This method, combined with real-time identification capabilities, lays the groundwork for efficient utilization of data from future solar observatories like the Advanced Space-based Solar Observatory (ASO-S).

The research in (Sukarsih et al., 2020) focused on the automatic detection of sunspots on the solar disc using images obtained from the SDO/AIA. The primary goal was to analyze solar activities, particularly sunspots, to enhance understanding and prediction of space weather. All processing was done in MATLAB. The method used for detection involved image processing techniques, including threshold segmentation and regionprops (MATLAB-based region detection algorithm), to compare the automatic detection results with NASA data from *solarmonitor.org*. The evaluation of results was conducted through coordinate validation using Root Mean Square Error (RMSE) to ensure accuracy and reliability in the detection process. Although this paper did both segmentation and detection, due to its primary goal for the detection of active regions, we put it in a sub-section related to detection approaches.

The detection process on the images obtained from the SDO/AIA involved several key steps. The images were initially in JPG format with a resolution of 512 x 512 pixels, representing the solar disc. The first step in the detection process was the transformation of the coloured images into greyscale to simplify the image to a grey level between 0 (black) and 255 (white). Following the greyscale conversion, the thresholding operation was performed to divide the grey into black and white, which helped to recognise and distinguish the main object, such as the active region or sunspots, from the background. This step was crucial in highlighting the bright areas that indicate the active region on the solar disc. Then, location and coordinates were identified using the regionprops MATLAB function which provided centroid value. The area was represented by a scalar value, while the centroid was expressed in coordinate form. The values of the area and centroid of the sunspots were analysed to further refine the detection process. However, both detection and segmentation did not show very good results.

In (Gong et al., 2024), the authors presented the deep learning architecture for the detection and tracking of active regions. They developed a novel deep learning method, ReDetGraphTracker, which is made up of two parts, detection and tracking modules. The detection module consists of the base detection module and the redetection module. The base detection module is based on DLA-34 encoder-decoder and was used as a Resnet-18-based redetection module to improve the performance of the base module in cases of missing detections during tracking. Models were trained on HMI and MDI magnetograms.

Other approaches - translation or generation techniques

This section explores the innovative methods utilized in recent studies to enhance, generate, and translate images of the solar corona. These techniques represent a significant departure from traditional detection and segmentation methods, focusing instead on leveraging advanced neural network models for image manipulation and generation. The studies highlighted in this section utilise a variety of data sources, primarily from the SDO, to address the challenges of high-resolution solar imaging and the translation of solar images across different wavelengths or instruments.

The paper (Giger and Csillaghy, 2024) introduces a method for identifying and localizing abnormal regions in solar images without the need for manual labeling or supervision. The authors used the SDO

machine learning data set (SDO ML) version 1[3], as published by (Galvez et al., 2019). This dataset contains a collection of solar images captured by the SDO satellite, which spans from 2010 to 2018 and provides spatially co-registered and corrected images suitable for machine learning analysis. The paper focuses on detecting and localising abnormal regions in solar images. These abnormal regions could represent various anomalies or irregularities in the solar corona, such as flares, prominences, coronal holes, or other unusual features.

To achieve this, the authors employed a variational autoencoder (VAE), a neural network architecture that combines variational inference with autoencoding. This approach allows the model to learn a representation of the data distribution and generate new data points similar to the training set. The results of the study likely demonstrated the effectiveness of the VAE-based unsupervised anomaly detection method in identifying and localizing abnormal regions in solar images.

One potential limitation of the study could be the complexity and interpretability of the VAE model. While VAEs are adept at capturing complex data distributions, their decision-making process may lack transparency, posing challenges in understanding how anomalies are detected.

Another study (Salvatelli et al., 2022) presents the aforementioned SDO-ML dataset to explore the creation of synthetic solar EUV images through image-to-image translation.

Their research focused on detecting morphological traits and brightness variations on the solar corona using a U-Net mode. The model aimed to reproduce the covariance across different EUV channels within a 1% error, emphasising the impact of solar surface traits on the network's predictions.

The results of the study showcased the model's ability to generate high-quality synthetic solar corona images across a broad range of pixel intensities, maintaining accuracy within an error margin of 1% for channel covariance. However, the model faced limitations in accurately reproducing rare and high-energy events such as solar flares, indicating challenges in training machine learning algorithms on such infrequent occurrences.

In the study (Dash et al., 2022), the researchers used SDO data accessed through the Joint Science Operations Centre (JSOC) server. They used pairs of SDO/AIA0304 images and SDO/HMI magnetograms to train their deep learning model. The objective of the study was to generate high-resolution SDO/AIA0304 images from SDO/HMI LOS magnetograms to detect structures on the solar corona such as coronal loops, filaments, coronal holes, and active regions.

To achieve this, the authors implemented conditional Generative Adversarial Networks, specifically utilising the Pix2PixHD and Pix2Pix models. These models were chosen for their effectiveness in image-to-image translation tasks, enabling the generation of high-resolution solar images from magnetogram data.

The results of the study demonstrated the successful generation of high-resolution solar images using GANs. Using Pix2PixHD and Pix2Pix algorithms, the researchers were able to translate SDO/HMI magnetograms into SDO/AIA0304 images, contributing to advancements in space weather prediction and solar event forecasting.

In (Jarolim et al., 2024) the authors use data from multiple instruments, including the SOHO, STEREO and the SDO. They focus on enhancing EUV images to SDO quality and calibrating them into a unified series dating back to 1996. The structures on the solar corona that they detect include filaments, solar limb features, quiet Sun regions, active regions, and magnetic elements such as sunspots.

The algorithm used in the paper involves a two-network neural network architecture. The first network generates synthetic low-quality images from high-quality images, while the second network is trained to invert the image degradation to reconstruct the original high-quality observation. Competitive training between the two generators and a discriminator network is employed to enforce the generation of low-quality images. In addition, a noise factor is included to model various degrading effects independent of image content. The cycle of translating low-quality observations to high-quality observations enforces that the images correspond to the domain of high-quality images.

The results of the study show a strong resolution increase and a high similarity to real reference observations. The method successfully enhances images, reconstructs faint features, and provides consistent results across the full solar disk. However, limitations include the inability to fully reconstruct smaller features, reach full HMI quality in magnetic elements, and resolve magnetic flux elements at the lowest resolution level. The method also has challenges in dealing with pixel errors and may not capture all the details present in the original high-quality images.

[3]https://sdoml.github.io/

In (Cherti et al., 2023) the authors used a subset of EUV images from the SDO/AIA instrument. The dataset consisted of high-resolution solar images capturing various structures in the solar corona, including coronal holes, active regions, and closed coronal loops with fine-scale details. The researchers used generative models, specifically exploring StyleGAN-based methods and diffusion-based generative models. Additionally, ProjectedGANs were utilised, incorporating multiscale discriminators with a pre-trained frozen feature extractor to enhance fine-scale detail generation.

Results from the study indicated that while StyleGAN-based methods struggled with fine-scale details of high-resolution solar images, diffusion-based generative models showed significant improvements in generating fine-scale structures. ProjectedGANs demonstrated enhanced performance in fine-scale detail generation, with the ability to train models up to 1024×1024 resolution, producing high-quality samples indistinguishable from human experts.

However, the study acknowledged limitations such as restricted resolution of the data set, which required a custom data preparation routine for high-resolution learning. Furthermore, the paper highlighted the underexplored area of unconditional noise-to-image synthesis in solar physics, suggesting potential avenues for future research. Although the research showcased advances in generative models for high-resolution solar imaging, further investigations may be required to fully realise the potential of these models in solar physics applications.

DISCUSSION AND CONCLUSION

In this paper, we provided an overview of segmentation techniques, both in general with an emphasis on deep learning approaches, and also specifically for the use of machine learning techniques in solar atmosphere structure segmentation and detection from recent years, which were used for corona holes, active regions, and sunspots. For the purpose of an overview, we used the methodology for acquisition of related papers and their approaches (algorithms). The overview of recent approaches shows that use of deep learning approaches have increased during last years and it is dominant in application in solar structures segmentation and detection now. We also have to mention that we included detection approaches and the approaches for generation/translation approaches. The reason is that in both cases it can be interesting to explore novel ideas that can be reused in different tasks, such as segmentation or detection. We can summarise the main findings of this survey and their consequences as follows.

- Deep learning approaches showed their strength in all the articles analysed. Moreover, generative approaches also show a lot of potential, one of the generative (translation) models known as Pix2Pix (version of conditional GAN) provides an interesting enhancement of the original U-Net, when U-Net is used as generator and PatchGAN as discriminator. Also, there are new algorithms which combine possibility for detection and segmentation in one architecture, example of which are newer YOLO models.
- As we have already seen, approximately half of the approaches used more input sources (such as different wavelengths, magnetograms, etc.) in their effort to achieve better results. It shows its importance in some approaches for reducing the number of false positive cases, e.g., to not segment filaments in coronal holes segmentation. However, the decision on whether more inputs (and which of them) are required instead of just one (which is always used, e.g., 193Å in SDO data for coronal holes) is up to the domain experts.
- The learning process requires the creation of training, validation, and testing datasets, as is expected for the evaluation of deep learning models. Evaluation procedures should follow standard segmentation metrics, which are pixel-based, such as IoU and Dice. However, due to the fact that annotation and ground truth might be considered as not exact (which is quite common in this domain), use of other evaluation techniques should be considered, such as qualitative visual inspection of segmentation results (by domain experts) or semi-qualitative evaluation based on the inspection of segmented areas and their comparison to labelling of these areas, which may lead to classification-like metrics based on confusion matrix evaluation.

REFERENCES

Abdulateef, S. K. and Salman, M. D. (2021). A comprehensive review of image segmentation techniques. *Iraqi Journal for Electrical & Electronic Engineering*, 17(2).

Almahasneh, M., Paiement, A., Xie, X., and Aboudarham, J. (2022). MSMT-CNN for solar active region detection with multi-spectral analysis. *SN Computer Science*, 3.

Arish, S., Javaherian, M., Safari, H., and Amiri, A. (2016). Extraction of active regions and coronal holes from EUV images using the unsupervised segmentation method in the bayesian framework. *Solar Physics*, 291(4):1209 – 1224.

Aschwanden, M. J. (2010). Image Processing Techniques and Feature Recognition in Solar Physics. *Solar Physics*, 262(2):235–275.

Baek, J.-H., Kim, S., Choi, S., Park, J., and Kim, D. (2024). Deep learning-based solar image captioning. *Advances in Space Research*, 73.

Baek, J.-H., Kim, S., Choi, S., Park, J., Kim, J., Jo, W., and Kim, D. (2021). Solar event detection using deep-learning-based object detection methods. *Solar Physics*, 296(11):160.

Bandyopadhyay, S., Das, S., and Datta, A. (2020a). Detection of coronal holes using Hough simulated Parameterized Online Region-based Active Contour Method. *2020 URSI Regional Conference on Radio Science, URSI-RCRS 2020 - Proceedings*, pages 1–4.

Bandyopadhyay, S., Das, S., and Datta, A. (2020b). Fuzzy energy-based dual contours model for automated coronal hole detection in SDO/AIA solar disk images. *Advances in Space Research*, 65(10):2435 – 2455.

Boucheron, L., Valluri, M., and McAteer, R. (2016). Segmentation of coronal holes using active contours without edges. *Solar Physics*, 291(8):2353 – 2372.

Camporeale, E., Wing, S., and Johnson, J. (2018). *Machine Learning Techniques for Space Weather*. Elsevier.

Canny, J. (1986). A computational approach to edge detection. *IEEE Transactions on Pattern Analysis and Machine Intelligence*, (6):679–698.

Caplan, R., Downs, C., and Linker, J. (2016). Synchronic coronal hole mapping using multi-instrument EUV images: Data preparation and detection method. *Astrophysical Journal*, 823(1).

Caplan, R. M., Mason, E. I., Downs, C., and Linker, J. A. (2023). Improving coronal hole detections and open flux estimates. *Astrophysical Journal*, 958(1).

Chen, L.-C., Papandreou, G., Schroff, F., and Adam, H. (2017). Rethinking atrous convolution for semantic image segmentation. *arXiv preprint arXiv:1706.05587*.

Chen, L.-C., Zhu, Y., Papandreou, G., Schroff, F., and Adam, H. (2018). Encoder-Decoder with atrous separable convolution for semantic image segmentation. In *Proceedings of the European Conference on Computer Vision (ECCV)*, pages 801–818.

Cherti, M., Czernik, A., Kesselheim, S., Effenberger, F., and Jitsev, J. (2023). A comparative study on generative models for high resolution solar observation imaging. *arXiv preprint arXiv:2304.07169*.

Çiçek, Ö., Abdulkadir, A., Lienkamp, S. S., Brox, T., and Ronneberger, O. (2016). 3D U-Net: learning dense volumetric segmentation from sparse annotation. In *Medical Image Computing and Computer-Assisted Intervention–MICCAI 2016: 19th International Conference, Athens, Greece, October 17-21, 2016, Proceedings, Part II 19*, pages 424–432. Springer.

Dash, A., Ye, J., Wang, G., and Jin, H. (2022). High resolution solar image generation using generative adversarial networks. *Annals of Data Science*, pages 1–17.

Delouille, V., Hofmeister, S. J., Reiss, M. A., Mampaey, B., Temmer, M., and Veronig, A. (2018). Coronal holes detection using supervised classification. *Machine Learning Techniques for Space Weather*, page 365 – 395.

Foullon, C. and Verwichte, E. (2006). Automated detection of EUV prominences. *Solar Physics*, 234(1):135–150.

Fox, N. J., Velli, M. C., Bale, S. D., Decker, R., Driesman, A., Howard, R. A., Kasper, J. C., Kinnison, J., Kusterer, M., Lario, D., Lockwood, M. K., McComas, D. J., Raouafi, N. E., and Szabo, A. (2016). The solar probe plus mission: Humanity's first visit to our star. *Space Science Reviews*, 204(1):7–48.

Gadari, A., Chandra Bollepalli, S., Ibrahim, M. N., Jose´-Alian, S., Chhablani, J., Suthaharan, S., and Kumar Vupparaboina, K. (2023). Robust retinal layer segmentation using OCT B-Scans: A novel approach based on Pix2Pix Generative Adversarial Network. In *Proceedings of the 14th ACM International Conference on Bioinformatics, Computational Biology, and Health Informatics*, BCB '23.

Galvez, R., Fouhey, D. F., Jin, M., Szenicer, A., Muñoz-Jaramillo, A., Cheung, M. C., Wright, P. J., Bobra, M. G., Liu, Y., Mason, J., et al. (2019). A machine-learning data set prepared from the NASA Solar Dynamics Observatory mission. *The Astrophysical Journal Supplement Series*, 242(1):7.

Garton, T. M., Gallagher, P. T., and Murray, S. A. (2018). Automated coronal hole identification via multi-thermal intensity segmentation. *Journal of Space Weather and Space Climate*, 8:A02.

Giger, M. and Csillaghy, A. (2024). Unsupervised anomaly detection with variational autoencoders applied to full-disk solar images. *Space Weather*, 22(2):e2023SW003516.

Gong, L., Yang, Y., Feng, S., Dai, W., Liang, B., and Xiong, J. (2024). Solar active regions detection and tracking based on deep learning. *Solar Physics*.

Goodfellow, I., Pouget-Abadie, J., Mirza, M., Xu, B., Warde-Farley, D., Ozair, S., Courville, A., and Bengio, Y. (2014). Generative Adversarial Nets. *Advances in Neural Information Processing Systems*, 27.

Grajeda, J. A., Boucheron, L. E., Kirk, M. S., Leisner, A., and Arge, C. N. (2023). Quantifying the consistency and characterizing the confidence of coronal holes detected by Active Contours Without Edges (ACWE). *Solar Physics*, 298(11).

Hamada, A., Asikainen, T., Virtanen, I., and Mursula, K. (2018). Automated identification of coronal holes from synoptic EUV maps. *Solar Physics*, 293(4):71.

He, K., Gkioxari, G., Dollár, P., and Girshick, R. (2017). Mask R-CNN. In *Proceedings of the IEEE International Conference on Computer Vision*, pages 2961–2969.

Heinemann, S. G., Temmer, M., Heinemann, N., Dissauer, K., Samara, E., Jerčić, V., Hofmeister, S. J., and Veronig, A. M. (2019). Statistical analysis and catalog of non-polar coronal holes covering the SDO-Era using CATCH. *Solar Physics*, 294(10).

Hughes, J. M., Hsu, V. W., Seaton, D. B., Bain, H. M., Darnel, J. M., and Krista, L. (2019). Real-time solar image classification: Assessing spectral, pixel-based approaches. *Journal of Space Weather and Space Climate*, 9:A38.

Ibtehaz, N. and Rahman, M. S. (2020). MultiResUNet: Rethinking the U-Net architecture for multimodal biomedical image segmentation. *Neural Networks*, 121:74–87.

Illarionov, E., Kosovichev, A., and Tlatov, A. (2020). Machine-learning approach to identification of coronal holes in solar disk images and synoptic maps. *Astrophysical Journal*, 903(2).

Illarionov, E. A. and Tlatov, A. G. (2018). Segmentation of coronal holes in solar disc images with a convolutional neural network. *Monthly Notices of the Royal Astronomical Society*, 481(4):5014–5021.

Inceoglu, F., Shprits, Y. Y., Heinemann, S. G., and Bianco, S. (2022). Identification of coronal holes on AIA/SDO images using unsupervised machine learning. *Astrophysical Journal*, 930(2).

Isola, P., Zhu, J.-Y., Zhou, T., and Efros, A. A. (2017). Image-to-image translation with conditional adversarial networks. In *Proceedings of the IEEE Conference on Computer Vision and Pattern Recognition*, pages 1125–1134.

Jarolim, R., Veronig, A. M., Hofmeister, S., Heinemann, S. G., Temmer, M., Podladchikova, T., and Dissauer, K. (2021). Multi-channel coronal hole detection with convolutional neural networks. *A&A*, 652:A13.

Jarolim, R., Veronig, A. M., Pötzi, W., and Podladchikova, T. (2024). Instrument-to-instrument translation: Instrumental advances drive restoration of solar observation series via deep learning. *arXiv preprint arXiv:2401.08057*.

Krista, L. D. and Gallagher, P. T. (2009). Automated coronal hole detection using local intensity thresholding techniques. *Solar Physics*, 256(1-2):87–100.

Krizhevsky, A., Sutskever, I., and Hinton, G. E. (2012). Imagenet classification with deep convolutional neural networks. *Advances in Neural Information Processing Systems*, 25.

Kucuk, A., Aydin, B., and Angryk, R. (2017). Multi-wavelength solar event detection using faster R-CNN. In *2017 IEEE International Conference on Big Data (Big Data)*, pages 2552–2558. IEEE.

Lecun, Y., Bengio, Y., and Hinton, G. (2015). Deep learning. *Nature*, 521(7553):436–444.

Lowder, C., Qiu, J., Leamon, R., and Liu, Y. (2014). Measurements of EUV coronal holes and open magnetic flux. *The Astrophysical Journal*, 783(2):142.

Mackovjak, Š., Harman, M., Maslej-Krešňáková, V., and Butka, P. (2021). SCSS-Net: solar corona structures segmentation by deep learning. *Monthly Notices of the Royal Astronomical Society*, 508(3):3111–3124.

Majirsky, A., Mackovjak, S., Kostarova, S., and Amrich, S. (2025). Extreme space weather events of the past 30 years: Preparation for data from mission vigil. *EARTH AND SPACE SCIENCE*, 12(2).

Mourato, A., Faria, J., and Ventura, R. (2024). Automatic sunspot detection through semantic and instance segmentation approaches. *Engineering Applications of Artificial Intelligence*, 129.

Müller, D., St. Cyr, O. C., Zouganelis, I., Gilbert, H. R., Marsden, R., Nieves-Chinchilla, T., Antonucci, E., Auchère, F., Berghmans, D., Horbury, T. S., Howard, R. A., Krucker, S., Maksimovic, M., Owen, C. J., Rochus, P., Rodriguez-Pacheco, J., Romoli, M., Solanki, S. K., Bruno, R., Carlsson, M., Fludra, A., Harra, L., Hassler, D. M., Livi, S., Louarn, P., Peter, H., Schühle, U., Teriaca, L., del Toro Iniesta, J. C., Wimmer-Schweingruber, R. F., Marsch, E., Velli, M., De Groof, A., Walsh, A., and Williams, D. (2020). The solar orbiter mission - science overview. *A&A*, 642:A1.

Oktay, O., Schlemper, J., Folgoc, L. L., Lee, M., Heinrich, M., Misawa, K., Mori, K., McDonagh, S., Hammerla, N. Y., Kainz, B., et al. (2018). Attention U-net: Learning where to look for the pancreas. *arXiv preprint arXiv:1804.03999*.

Palomba, M. and Luntama, J.-P. (2022). Vigil: Esa space weather mission in l5. *44th COSPAR Scientific Assembly. Held 16-24 July*, 44:3544.

Patel, K., Shah, P., and Gajjar, R. (2023). Semantic segmentation of urban area using Pix2Pix Generative Adversarial Networks. In *2023 3rd International Conference on Range Technology (ICORT)*, pages 1–6.

Pérez-Suárez, D., Higgins, P. A., Bloomfield, D. S., McAteer, R. T. J., Krista, L. D., Byrne, J. P., and Gallagher, P. T. (2011). *Automated Solar Feature Detection for Space Weather Applications*, pages 207–225. IGI Global.

Pesnell, W. D., Thompson, B. J., and Chamberlin, P. (2012). *The solar dynamics observatory (SDO)*. Springer.

Quan, L., Xu, L., Li, L., Wang, H., and Huang, X. (2021). Solar active region detection using deep learning. *Electronics*, 10(18):2284.

Redmon, J., Divvala, S., Girshick, R., and Farhadi, A. (2016). You Only Look Once: Unified, real-time object detection. In *Proceedings of the IEEE Conference on Computer Vision and Pattern Recognition*, pages 779–788.

Reiss, M. A., Muglach, K., Mason, E., Davies, E. E., Chakraborty, S., Delouille, V., Downs, C., Garton, T. M., Grajeda, J. A., Hamada, A., Heinemann, S. G., Hofmeister, S., Illarionov, E., Jarolim, R., Krista, L., Lowder, C., Verwichte, E., Arge, C. N., Boucheron, L. E., Foullon, C., Kirk, M. S., Kosovichev, A., Leisner, A., Möstl, C., Turtle, J., and Veronig, A. (2024). A Community Data Set for Comparing Automated Coronal Hole Detection Schemes. *Astrophysical Journal Supplement Series*, 271(1):6.

Reiss, M. A., Muglach, K., Möstl, C., Arge, C. N., Bailey, R., Delouille, V., Garton, T. M., Hamada, A., Hofmeister, S., Illarionov, E., Jarolim, R., Kirk, M. S. F., Kosovichev, A., Krista, L., Lee, S., Lowder, C., MacNeice, P. J., Veronig, A., and Cospar Iswat Coronal Hole Boundary Working Team (2021). The Observational Uncertainty of Coronal Hole Boundaries in Automated Detection Schemes. *Astrophysical Journal*, 913(1):28.

Ren, S., He, K., Girshick, R., and Sun, J. (2015). Faster R-CNN: Towards real-time object detection with region proposal networks. *Advances in Neural Information Processing Systems*, 28.

Ronneberger, O., Fischer, P., and Brox, T. (2015). U-Net: Convolutional networks for biomedical image segmentation. In *Medical image computing and computer-assisted intervention–MICCAI 2015: 18th international conference, Munich, Germany, October 5-9, 2015, proceedings, part III 18*, pages 234–241. Springer.

Roy, N., Kundu, A., Sikder, P., and Bhowmik, S. (2023). Lesion image segmentation for skin cancer detection using Pix2Pix: A deep learning approach. In *Proceedings of International Conference on Data, Electronics and Computing*, pages 303–311. Springer Nature Singapore.

Salvatelli, V., Dos Santos, L. F., Bose, S., Neuberg, B., Cheung, M. C., Janvier, M., Jin, M., Gal, Y., and Baydin, A. G. (2022). Exploring the limits of synthetic creation of solar EUV images via Image-To-Image translation. *The Astrophysical Journal*, 937(2):100.

Santos, J., Peixinho, N., Barata, T., Pereira, C., Coimbra, A. P., Crisóstomo, M. M., and Mendes, M. (2023). Sunspot detection using YOLOv5 in spectroheliograph H-alpha images. *Applied Sciences*, 13(10):5833.

Sarker, T. T. and Banda, J. M. (2019). Solar event tracking with deep regression networks: A proof of concept evaluation. In *2019 IEEE International Conference on Big Data*, pages 4942–4949.

Sayez, N., De Vleeschouwer, C., Delouille, V., Bechet, S., and Lefèvre, L. (2023). SunSCC: Segmenting, grouping and classifying sunspots from ground-based observations using deep learning. *Journal of Geophysical Research: Space Physics*, 128(12).

Sezgin, M. and Sankur, B. l. (2004). Survey over image thresholding techniques and quantitative

performance evaluation. *Journal of Electronic imaging*, 13(1):146–168.

Spogli, L. (2024). The effects of the may 2024 mother's day superstorm over the mediterranean sector: from data to public communication. *Authorea Preprints*.

Sukarsih, I., Hermawanti, A., Respitawulan, Priyatikanto, R., and Kurniati, E. (2020). Automatic detection process of solar active region based on SDO/AIA digital image. *Journal of Physics: Conference Series*, 1613(1).

van der Schot, A., Sikkel, E., Niekolaas, M., Spaanderman, M., and de Jong, G. (2023). Placental vessel segmentation using Pix2Pix compared to U-Net. *Journal of Imaging*, 9(10).

Verbeeck, C., Delouille, V., Mampaey, B., and De Visscher, R. (2014). The SPoCA-suite: Software for extraction, characterization, and tracking of active regions and coronal holes on EUV images. *A&A*, 561:A29.

Yan-mei, C., Si-qing, L., and Li-qin, S. (2021). Automatic recognition of solar active regions based on real-time SDO/HMI full-disk magnetograms. *Chinese Astronomy and Astrophysics*, 45:458–469.

Zaitoun, N. M. and Aqel, M. J. (2015). Survey on image segmentation techniques. *Procedia Computer Science*, 65:797–806.

Zhou, Z., Rahman Siddiquee, M. M., Tajbakhsh, N., and Liang, J. (2018). UNet++: A nested U-Net architecture for medical image segmentation. In *Deep Learning in Medical Image Analysis and Multimodal Learning for Clinical Decision Support: 4th International Workshop, DLMIA 2018, and 8th International Workshop, ML-CDS 2018, Held in Conjunction with MICCAI 2018, Granada, Spain, September 20, 2018, Proceedings 4*, pages 3–11. Springer.

Zhu, J.-Y., Park, T., Isola, P., and Efros, A. A. (2017). Unpaired image-to-image translation using cycle-consistent adversarial networks. In *Proceedings of the IEEE International Conference on Computer Vision*, pages 2223–2232.